Status Update on kronoseismology

ETHAN DEDERICK

JIVE MEETING

JUNE 26, 2017

Why Saturn & Not Jupiter?

1. We have the necessary observations to perform seismic inversions given a Saturn model

2. We're building the framework to capitalize on the measurements obtained from Jupiter

- Given recent Juno announcements, the planet model may be significantly different between Saturn and Jupiter

Mode Resonances

Unlike Jupiter (at least for now), we know which modes exist

ILR launched by satellite. Spiral density wave propagates away from the planet.

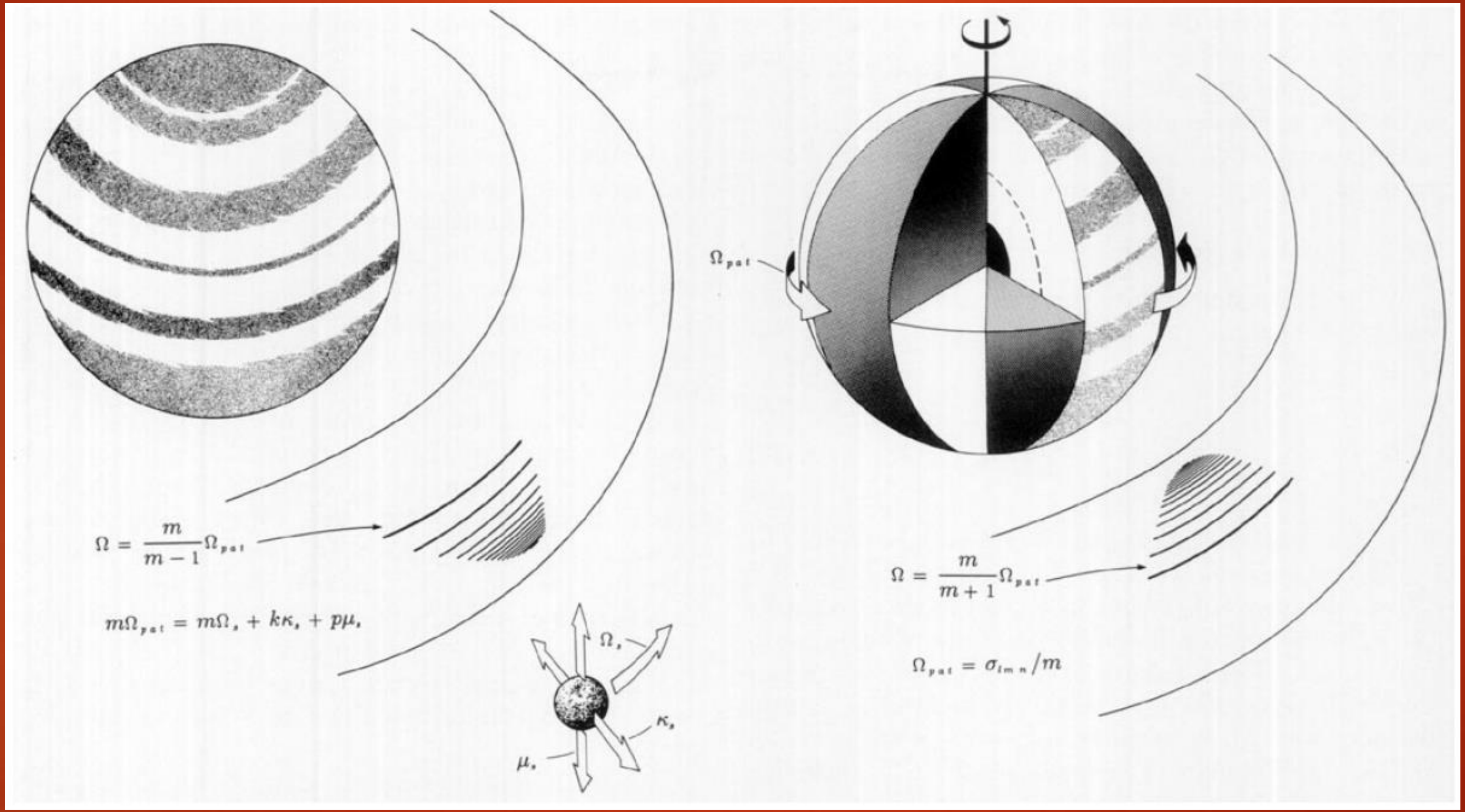

OLR launched by oscillation. Spiral density wave propagates toward the planet.

Taken from Marley & Porco 1993

Mode Resonances

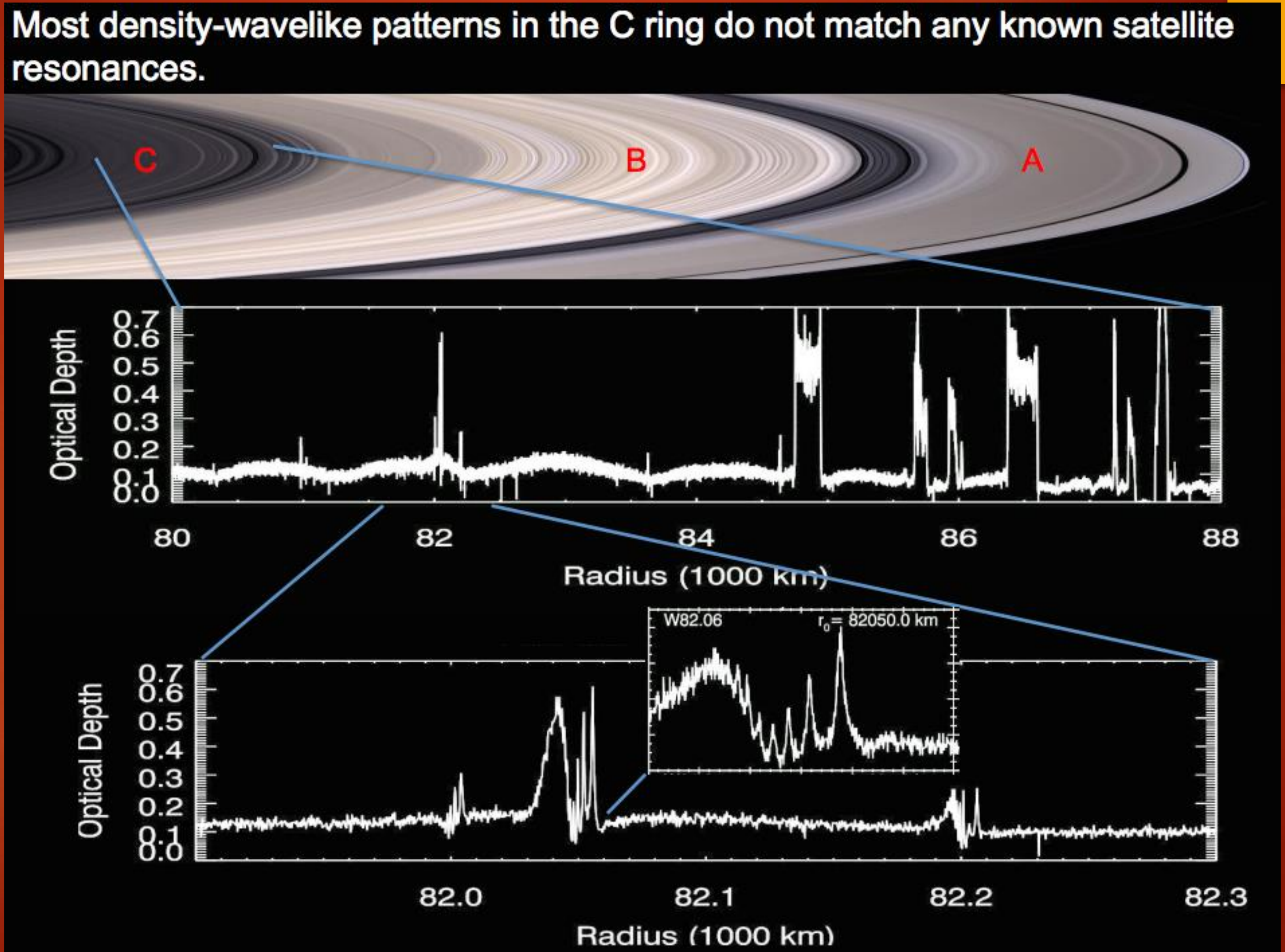

Taken from Nicholson & Hedman: Kronoseismology II

All Resonances

List of identified & unidentified waves in Saturn's C ring.

Baille no.	Rosen ID	HN13/14	a (res)	In/Out?	m value	pattern speed	res_type	source	notes	reference
1			74666	O	7	1725.8	OVR	f mode (10,7)?	bending wave?	RGF, CM
2	a		74892	O	2	763	ILR	Mimas 4:1		Rosen91, HN14
3			74933	O	4	1879.7	OVR	f mode (5,4)	bending wave?	RGF, CM
4	b		74941	O	9	1667.7	OVR	f mode (14,9)?	bending wave?	RGF, CM
5			76018	I	9	1626.5	OLR	f mode (13,9)		RGF, CM
6			76237	O	8	1645.4	OVR	f mode (11,8)?	bending wave?; within P1	RGF, CM
9			76438	I	2	2169.2	OLR	f mode (4,2)?		RGF, CM
			76460	I					alpAur (41)	
10			76539	?					narrow gap?	
11			76729	?					on peak; narrow gap?	
12	c		77520	O	1	22.577	IVR	Titan -1:0	bending wave; neg pat. Speed	RL88, NH16
13	e	W80.98	80988	I	4	1660.4	OLR	f mode (4,4)		HN13
14		W81.02	81024	I?					bending wave?	HN13 *
15		W82.01	82010	I	3	1736.6	OLR	f mode (3,3)		HN13
16	f	W82.06	82061	I	3	1735	OLR	f mode (3,3)		HN13
17	g	W82.21	82209	I	3	1730.3	OLR	f mode (3,3)		HN13
18	h	W83.63	83633	I	10	1394.1	OLR	f mode (10,10)		HN14
19	i	W84.64	84644	I	2	1860.8	OLR	f mode (2,2)		HN13
20		W84.82	84814	O	3	833.5	ILR	tesseral 3:2	within P5	HN14
21		W84.86	84857	O	3	833	ILR	tesseral 3:2	within P5	HN14
22			85105	?	2	606?	ILR	Pan 2:1		?
23	j		85450	I	3?		IVR?	tesseral 3:2	bending wave?	
24			85473	O						
25			85514	I	3?		IVR?	tesseral 3:2	bending wave?	
26			85523	O						
27	d	W85.67	85677	O	3?	810.2	IVR?	tesseral 3:2	bending wave?; within P6	HN14 **
28		W86.40	86400	O	3	810.4	ILR	tesseral 3:2	within P7	HN14
29		W86.58	86576	O	3	807.9	ILR	tesseral 3:2	within P7	HN14
31		W86.59	86590	O	3	807.7	ILR	tesseral 3:2	at edge of P7	HN14
32		W87.19	87193	I	2	1779.5	OLR	f mode (2,2)	on a peak	HN13
			87533	I	2	1769.15	OLR	f mode (2,2)	within Maxwell ringlet	French16
33			87647	O	2	598?	ILR	Atlas 2:1		?
34			88713	O?	2	587?	ILR	Prometheus 2:1	within Bond ringlet	
35			88736	O	1	14.03	ILR	Bond ringlet?	outside Bond gap	HN14
36			89883	O	3	763	ILR	Mimas 6:2	within P10	Baillie11, HN14
37			89894	O	3	762.85	ILR	Pandora 4:2	within P10	Baillie11, HN14
38			90156	?	2	572?	ILR	Pandora 2:1	within Dawes ringlet	

Goal

- To utilize theoretical models and observational mode frequencies to perform inversions

Optical Depth Variation

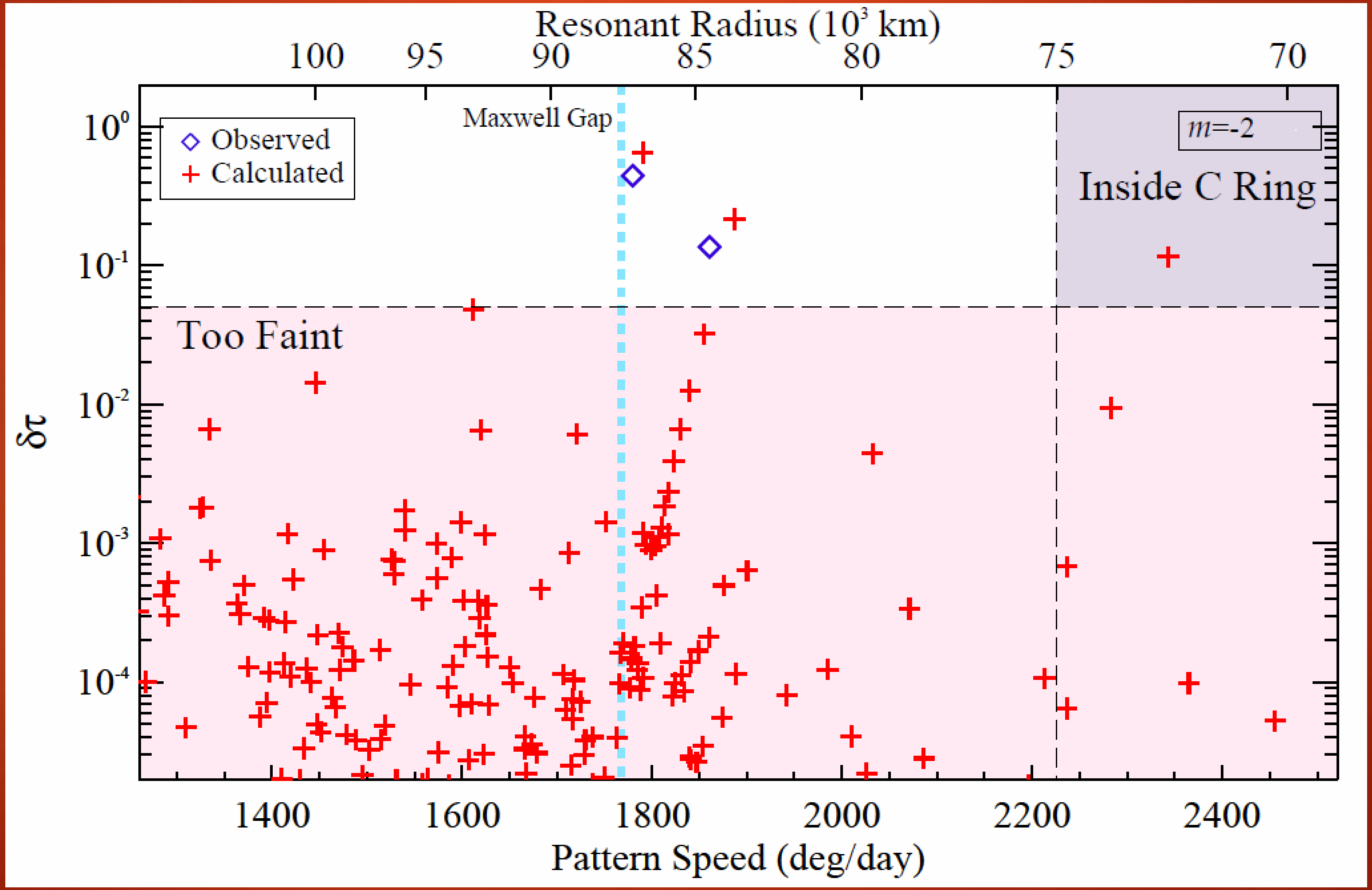

m = -2

Steps

1. Derive Kernel expressions
2. Create sophisticated Saturn model
3. Compute eigenfunctions and eigenfrequencies
4. Perform inversions
5. Check if the results are within acceptable errors
6. Repeat

Kernel Expressions

$$\frac{\delta\omega_{n,l}}{\omega_{n,l}} = \int_0^R \left[K_{nl}^{c,\rho}(r)\frac{\delta c}{c}(r) + K_{nl}^{\rho,c}(r)\frac{\delta\rho}{\rho}(r) \right] \mathrm{d}r$$

Kernel Expressions

$$\frac{\delta\omega_{n,l}}{\omega_{n,l}} = \int_0^R \left[K_{nl}^{c,\rho}(r)\frac{\delta c}{c}(r) + K_{nl}^{\rho,c}(r)\frac{\delta\rho}{\rho}(r) \right] \mathrm{d}r$$

$$K_{nl}^{c_s,\rho}(r) = \left(\omega^2 E_{nl} - 2i\omega\Omega_s \int\limits_0^R Z_s \rho r^2 dr \right)^{-1} \rho r^2 c_s^2 D_1^2$$

$$\begin{aligned}
K_{nl}^{\rho,c_s}(r) = {} & \left(\omega^2 E_{nl} - 2i\omega\Omega_s \int\limits_0^R Z_s \rho r^2 dr \right)^{-1} \rho r^2 \Bigg[-\frac{\omega^2}{2}\left(\tilde{\xi_r}^2 + l(l+1)\tilde{\xi_h}^2\right) + \frac{1}{2}c_s^2 D_1^2 \\
& + \frac{2Gm}{r^3}\tilde{\xi_r}\left[\tilde{\xi_r}\left(\frac{\pi\rho r^3}{m} - 1\right) + \frac{1}{2}l(l+1)\tilde{\xi_h}\right] \\
& - 4\pi G \int\limits_r^R \rho\tilde{\xi_r}\left[D_1 + \frac{1}{2}\tilde{\xi_r}\frac{\partial \ln\rho}{\partial r}\right] dr' \\
& - \frac{2\pi G}{2l+1}(l+1)r^{-l-2}\left(\tilde{\xi_r} - l\tilde{\xi_h}\right)\left(\int\limits_0^r D_2(r')r'^{l+2}dr'\right) \\
& + \frac{2\pi G}{2l+1}lr^{l-1}\left(\tilde{\xi_r} + (l+1)\tilde{\xi_h}\right)\left(\int\limits_r^R D_2(r')r'^{-l+1}dr'\right) \\
& - \frac{8\pi^2 G}{2l+1}\rho(R)\tilde{\xi_r}(R)\left(\frac{r}{R}\right)^{l-1} l\left(\tilde{\xi_r} + (l+1)\tilde{\xi_h}\right) + 2i\omega\Omega_s Z_s \Bigg]
\end{aligned}$$

Saturn Model

y-axis units are arbitrary

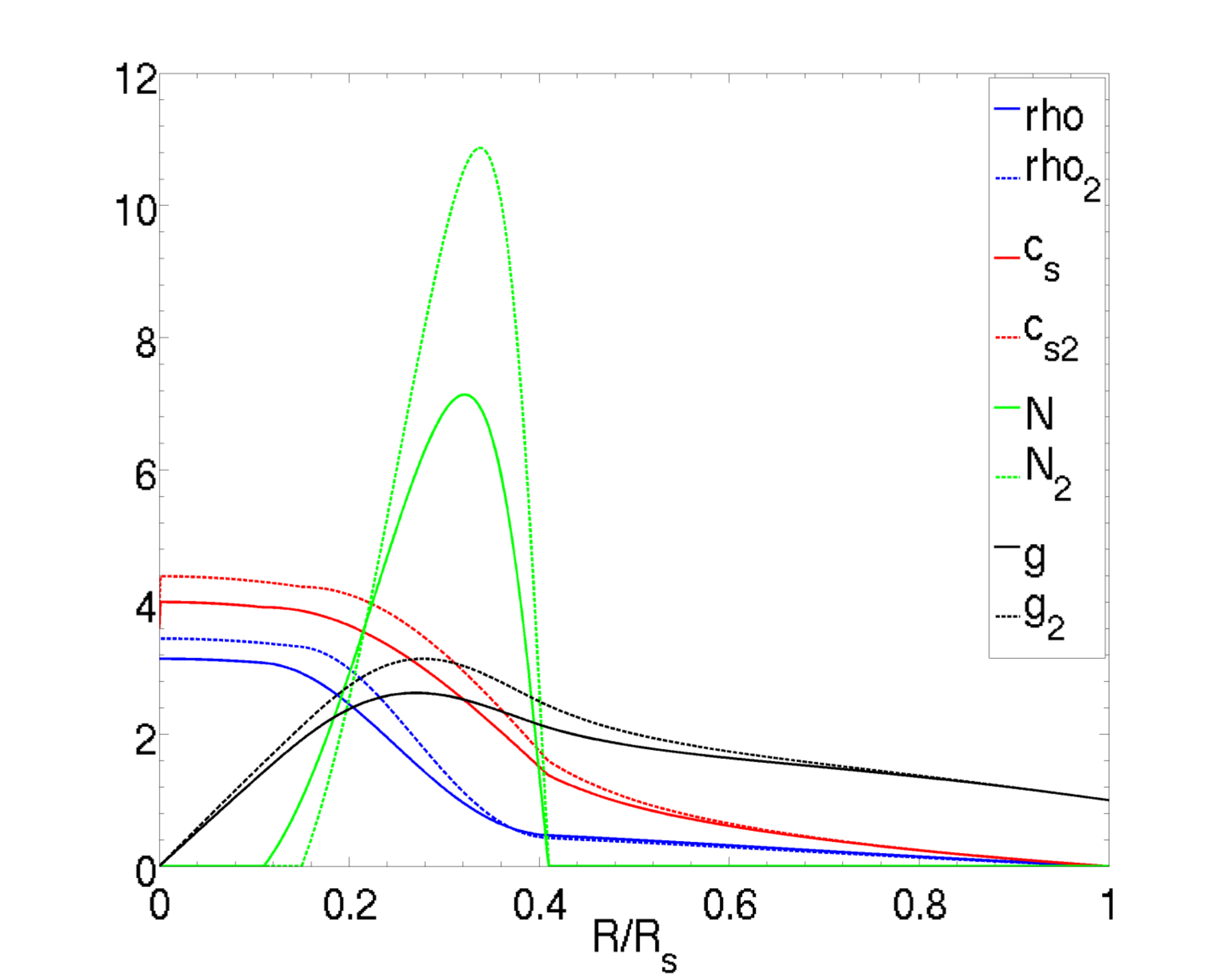

Eigenfunctions – Non-Rotating

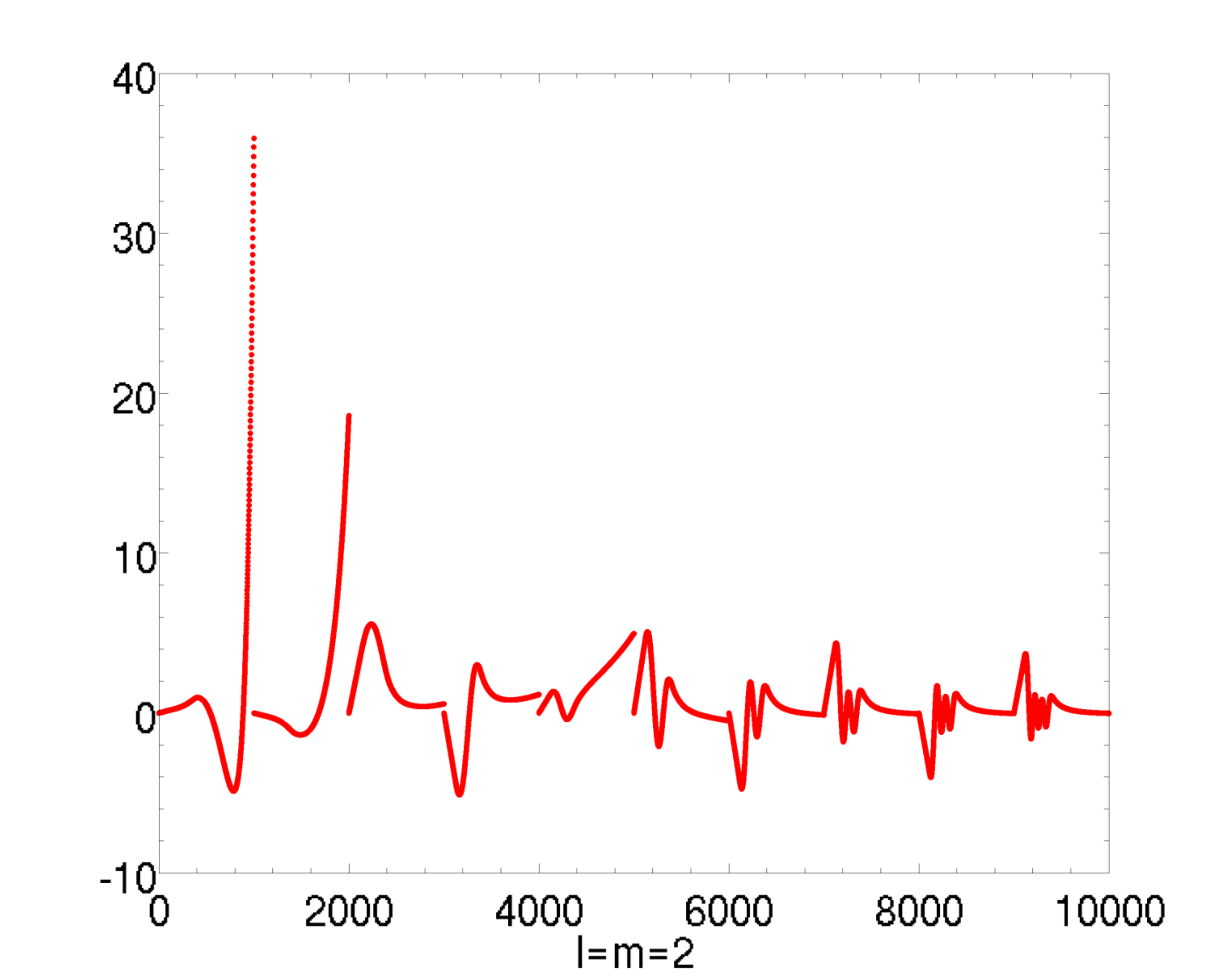

Eigenfunctions – Non-Rotating

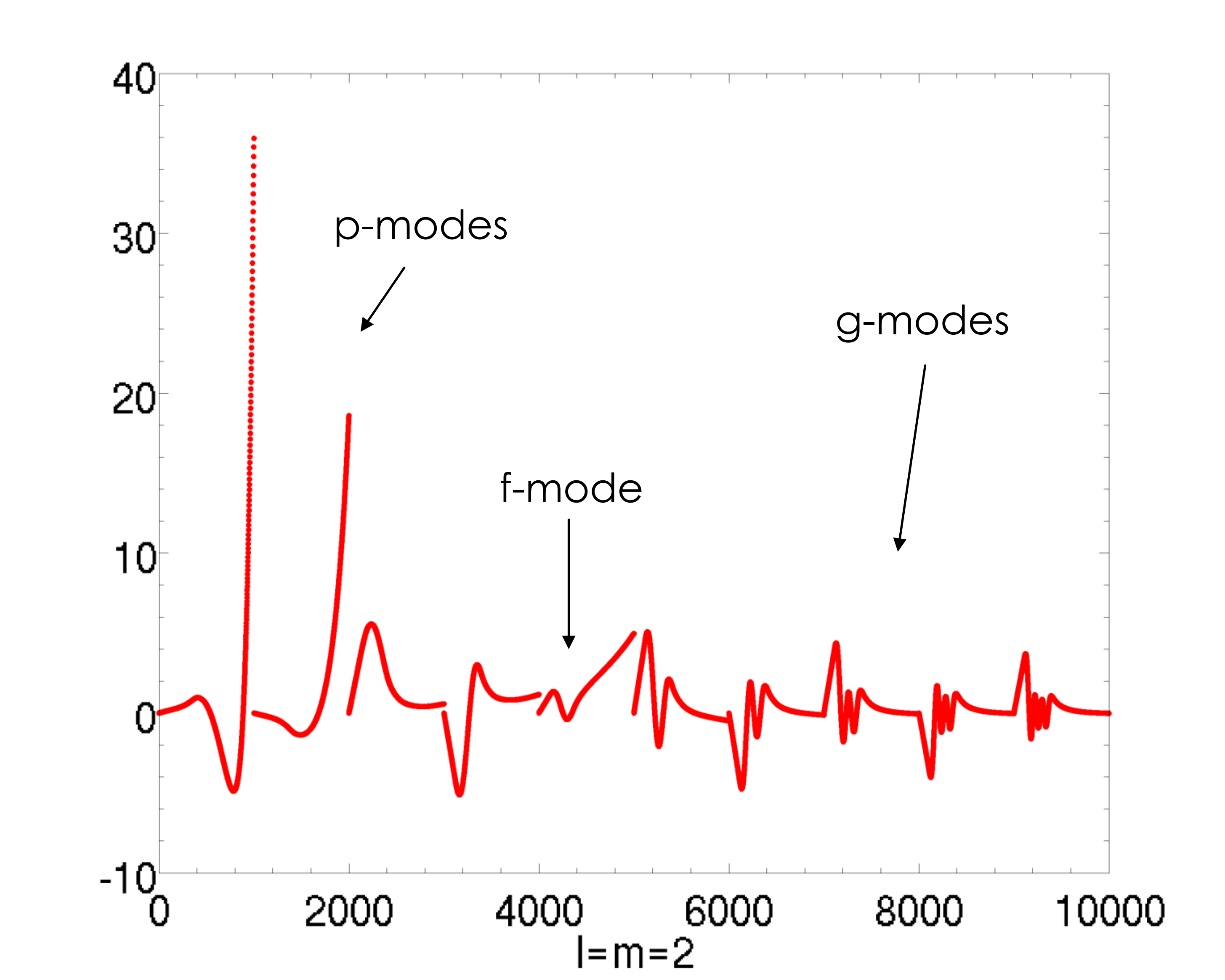

Mode mixing can occur without rotation if Brunt-Vaisala frequency is large enough to allow for g-modes of frequency close to that of f-modes

Eigenfunctions – Rotating (10 Hrs)

Before Rotational Mixing

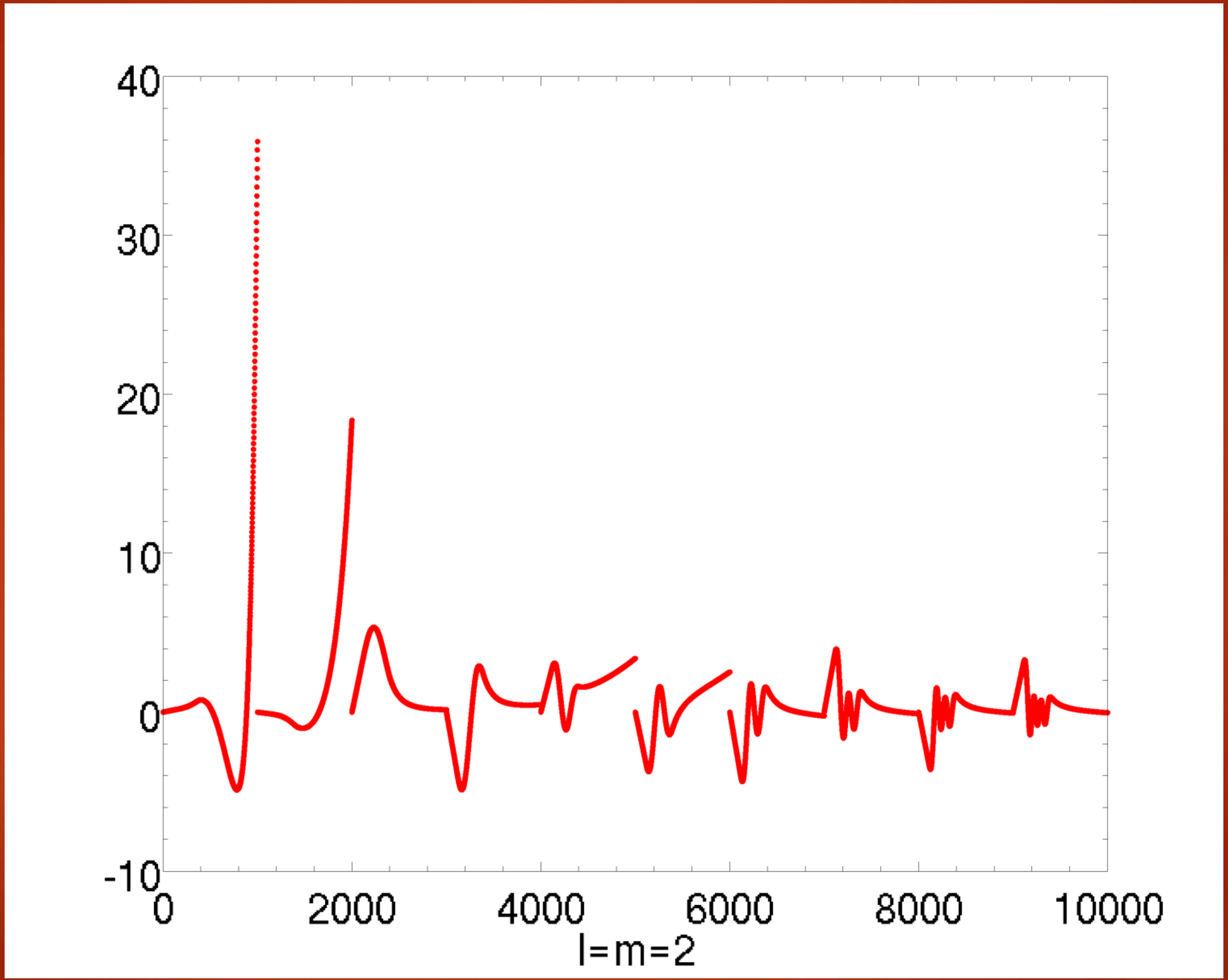

2 f-mode ring candidates – shows importance of Brunt – Vaisala frequency

Eigenfunctions – Rotating (10 Hrs)

After Rotational Mixing

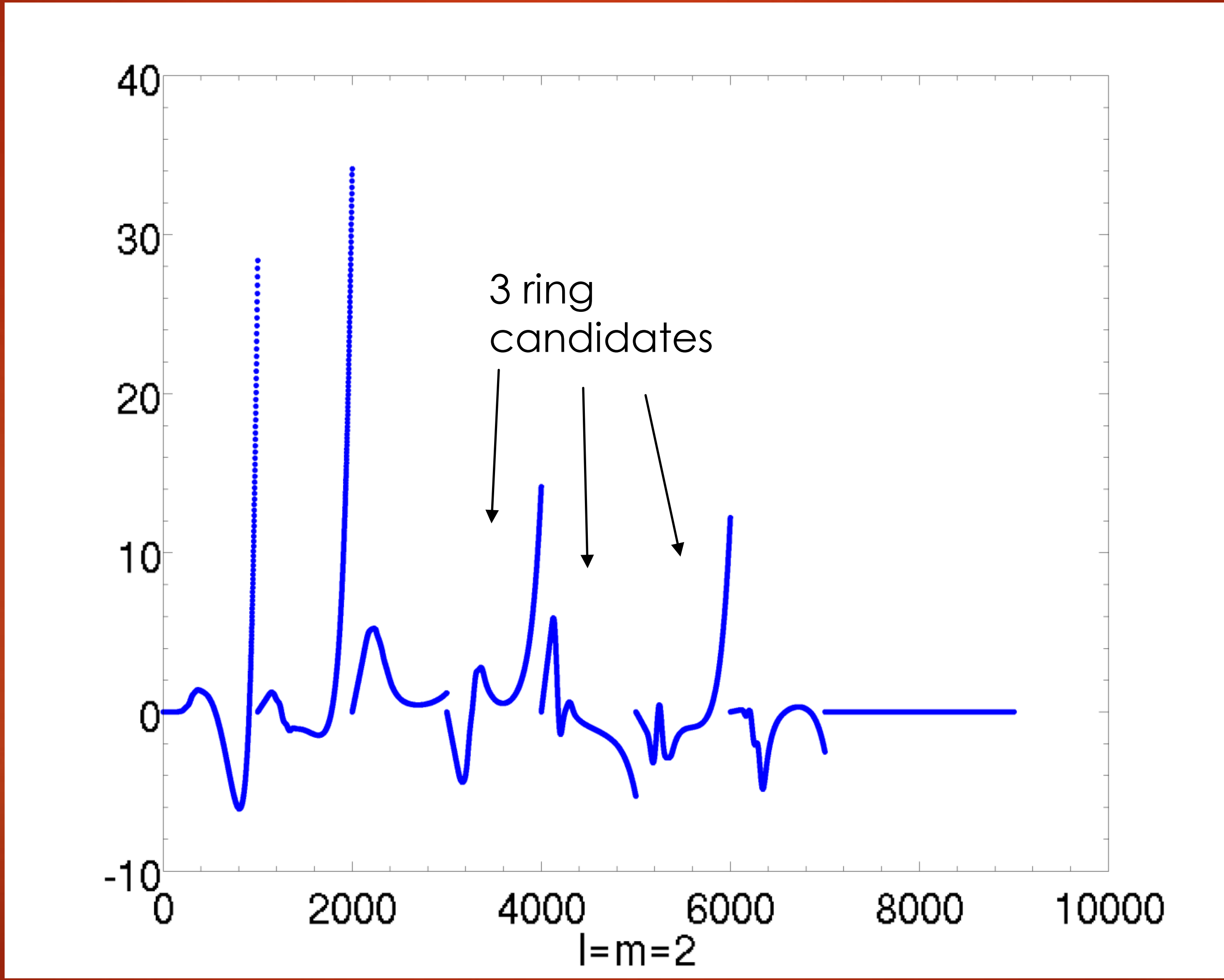

Mixing Coefficients – Non-Rotating

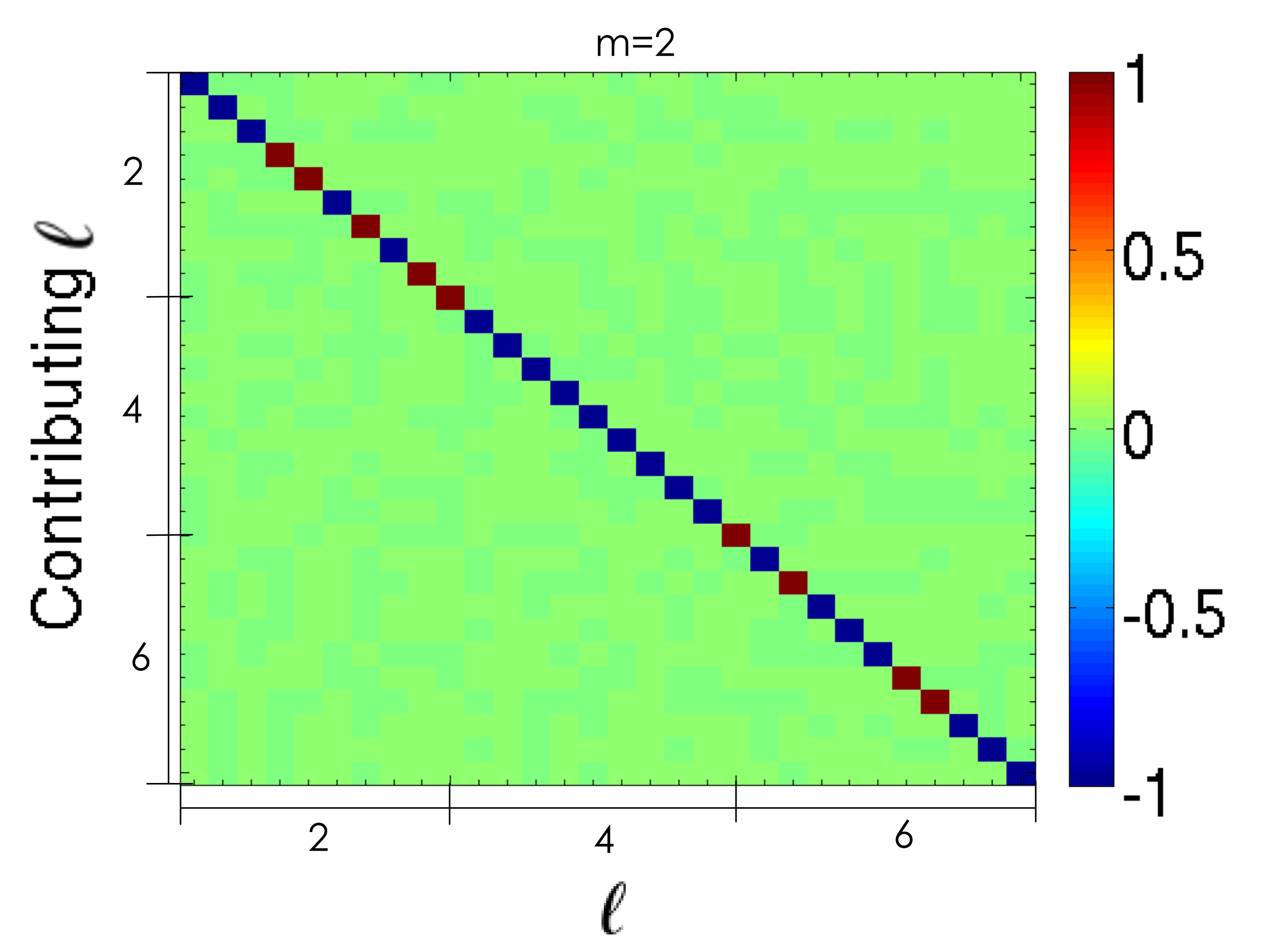

Mixing Coefficients – Rotating (10 Hrs)

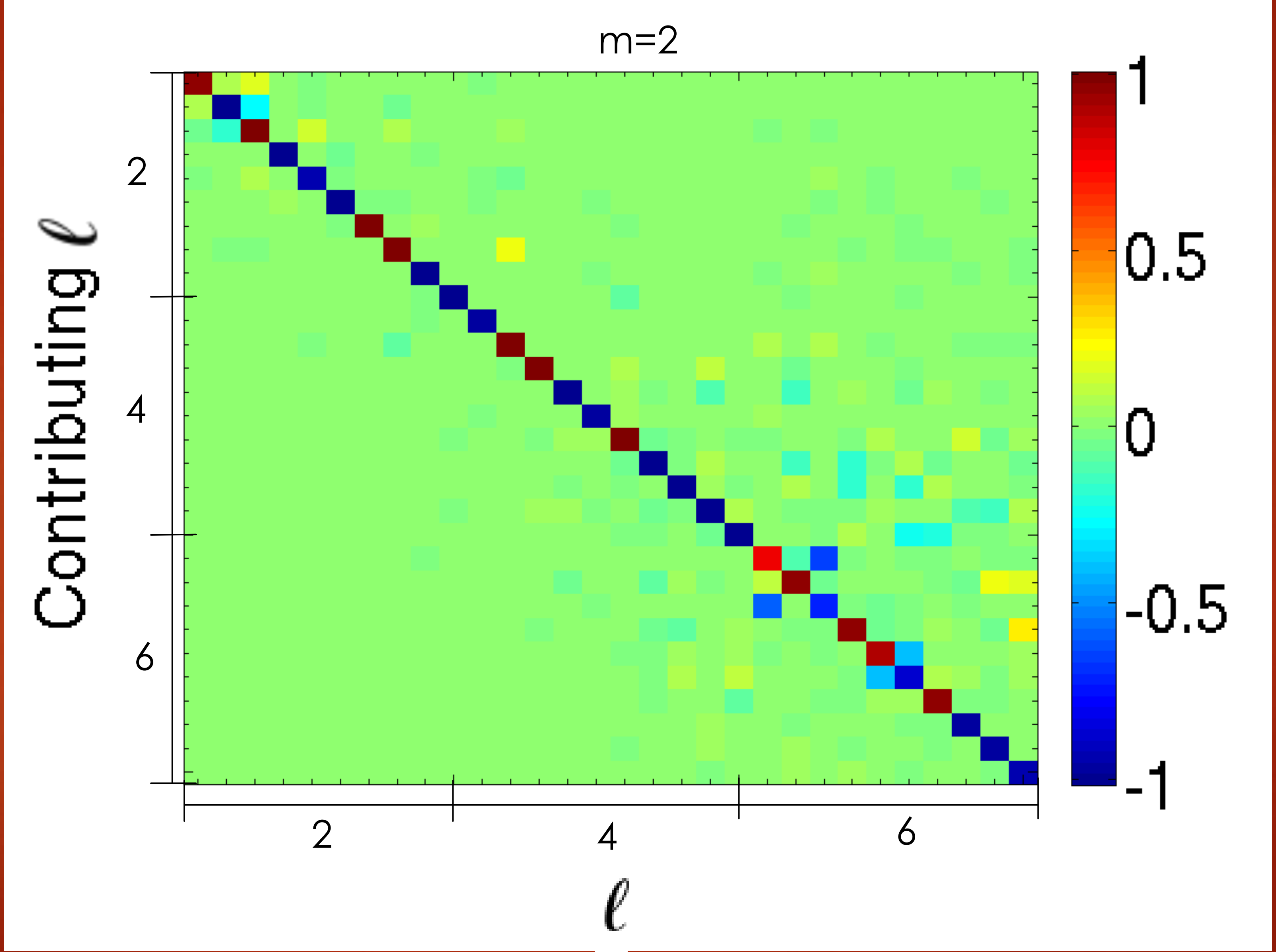

Mixing Coefficients – Rotating (10 Hrs)

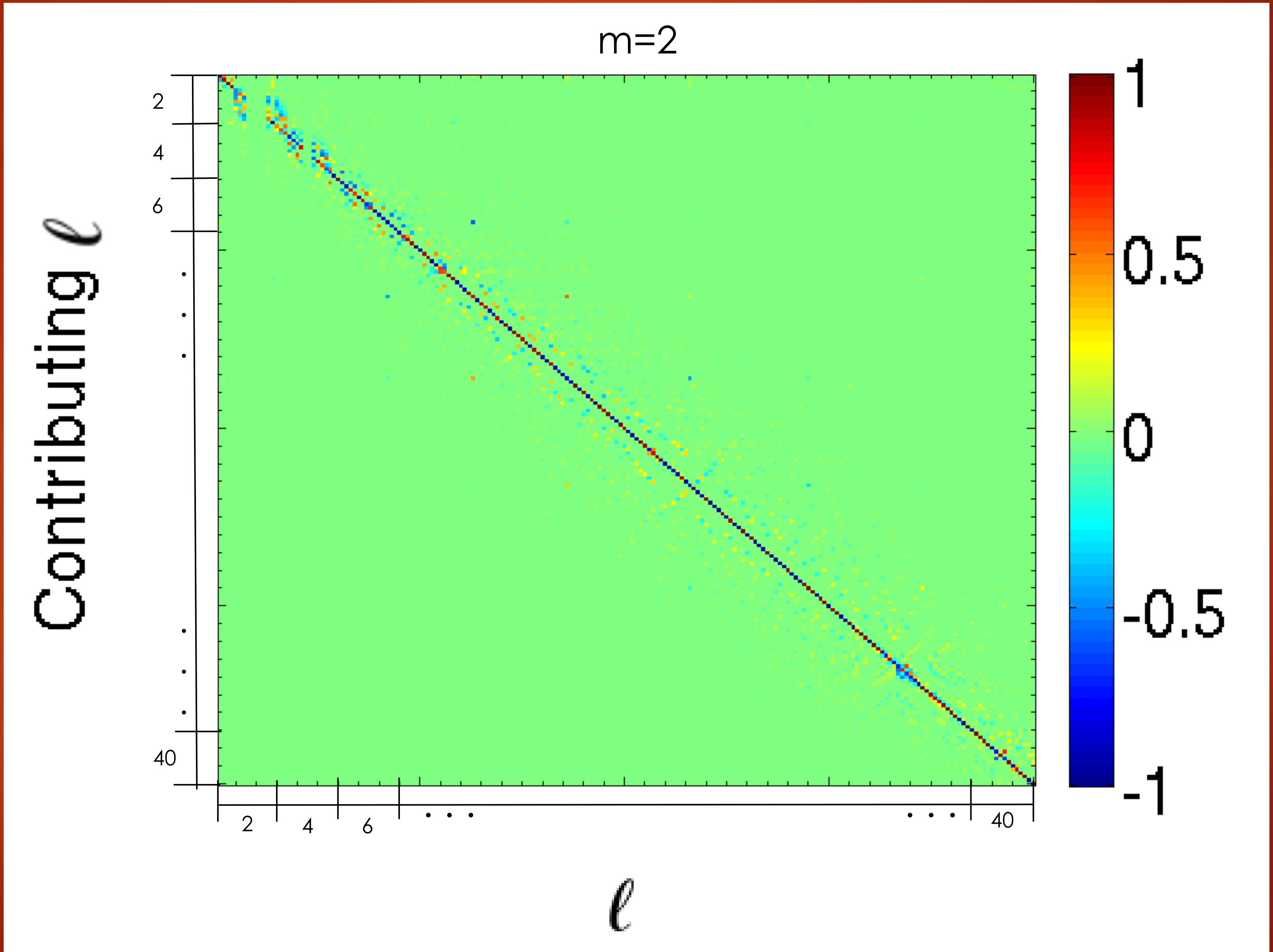

Kernels – f-modes

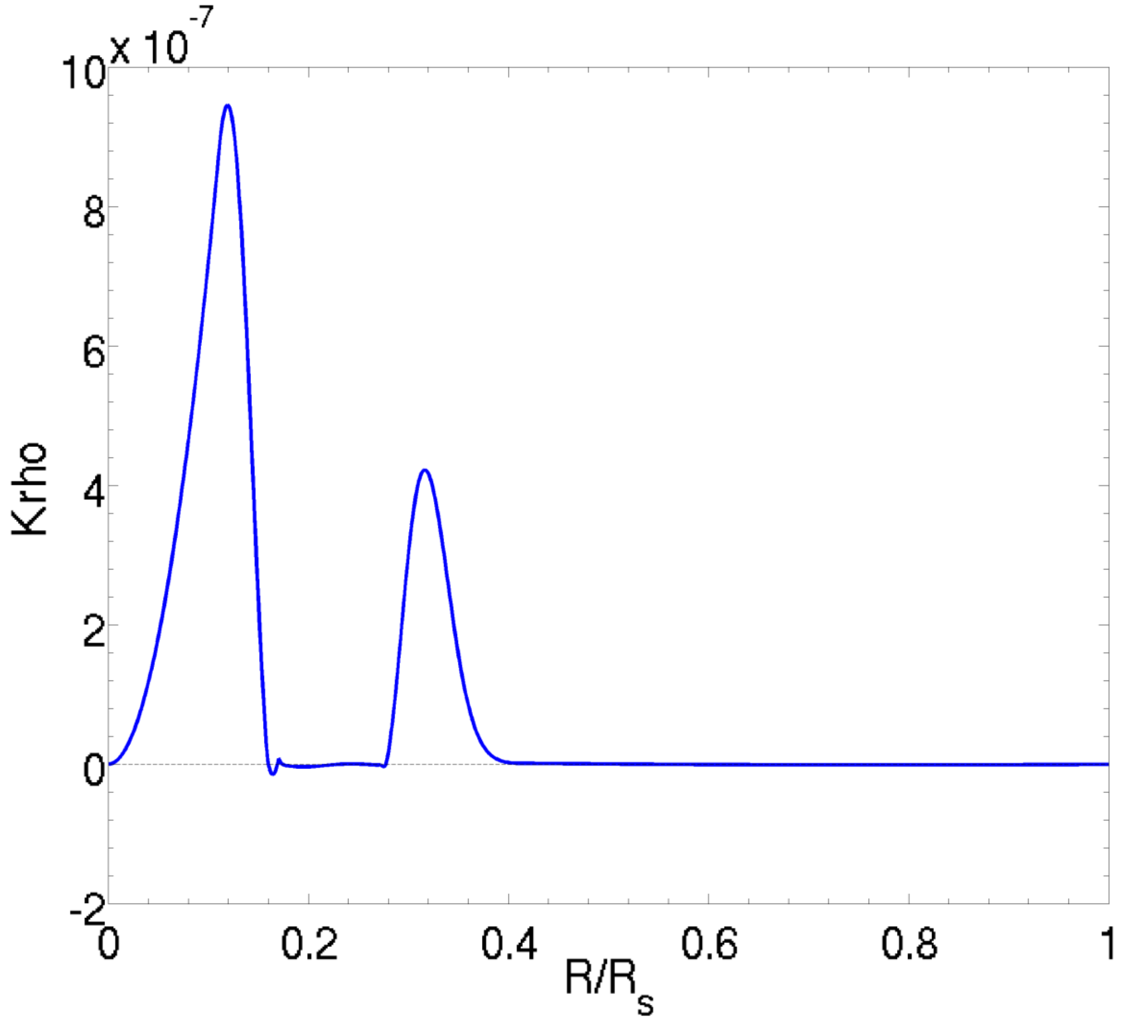

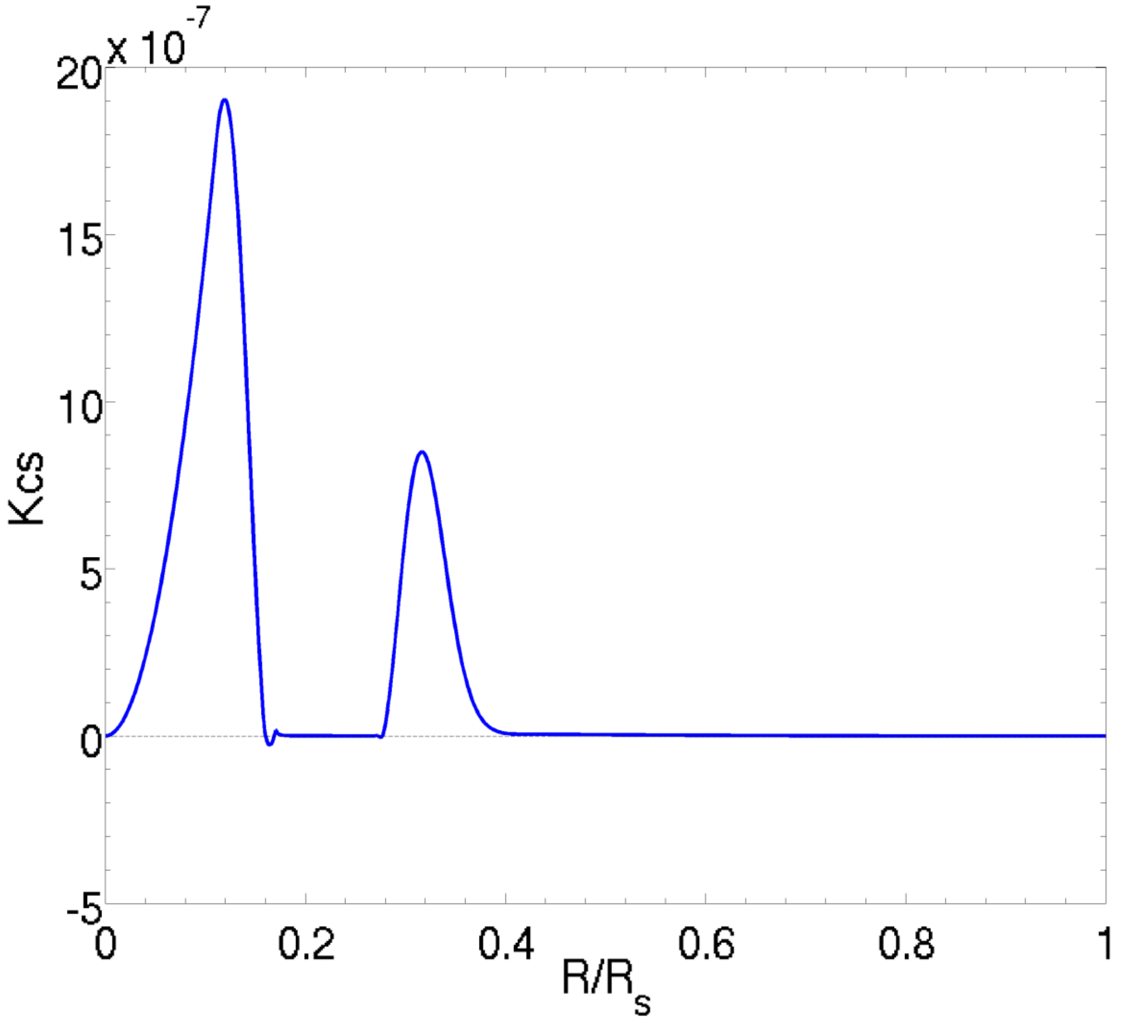

Kernels – other modes

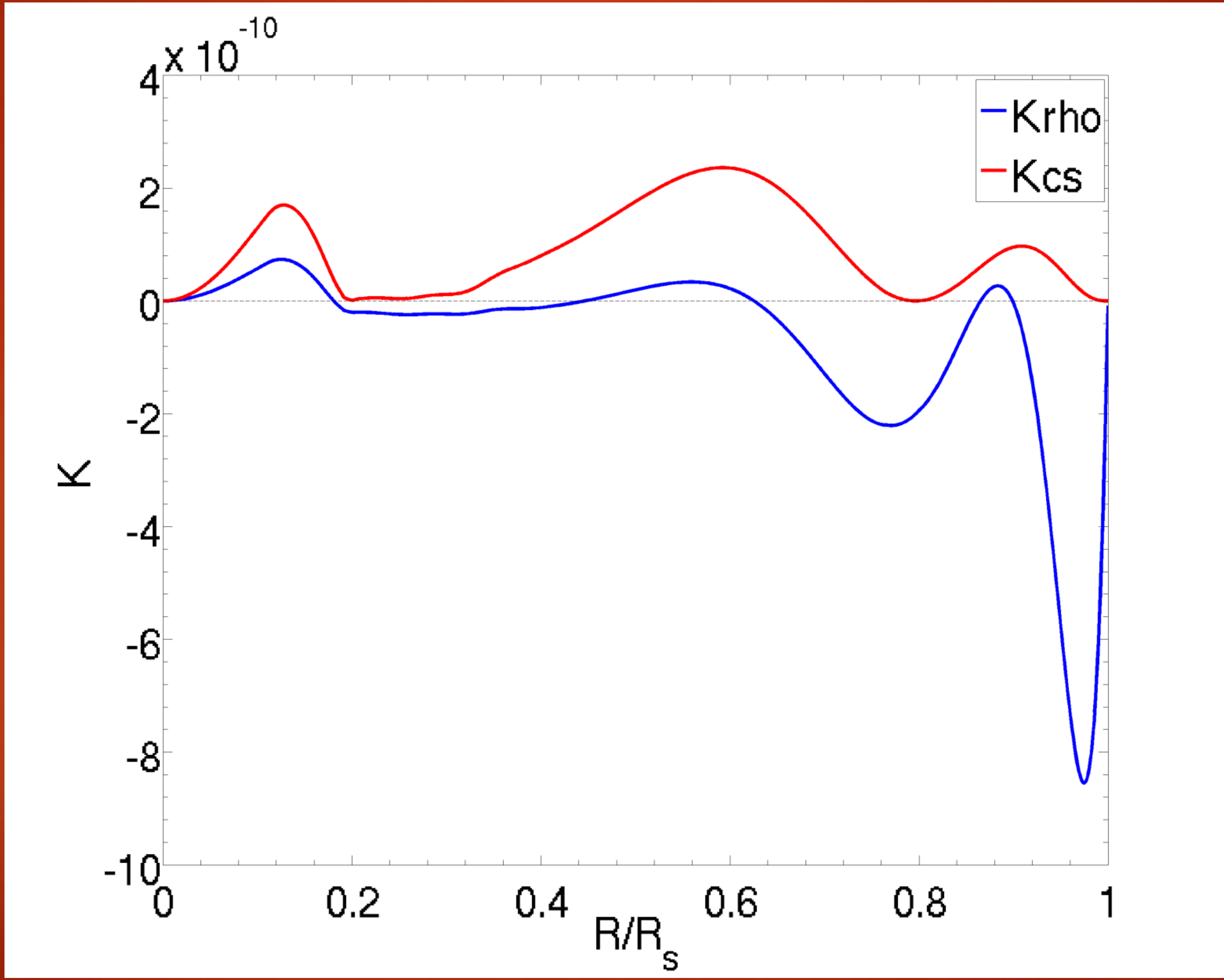

Future Work – Inversions

- Subtractive Optimally Localized Averages (SOLA) procedure
- Sum weighted kernels to match a target function at a specified radius

$$\overline{p}^{\alpha}(r_0) = \sum_{i=1}^{N} a_i^{\alpha}(r_0)\frac{\delta\omega_i}{\omega_i}$$

Taken from Jackiewicz et al. 2012

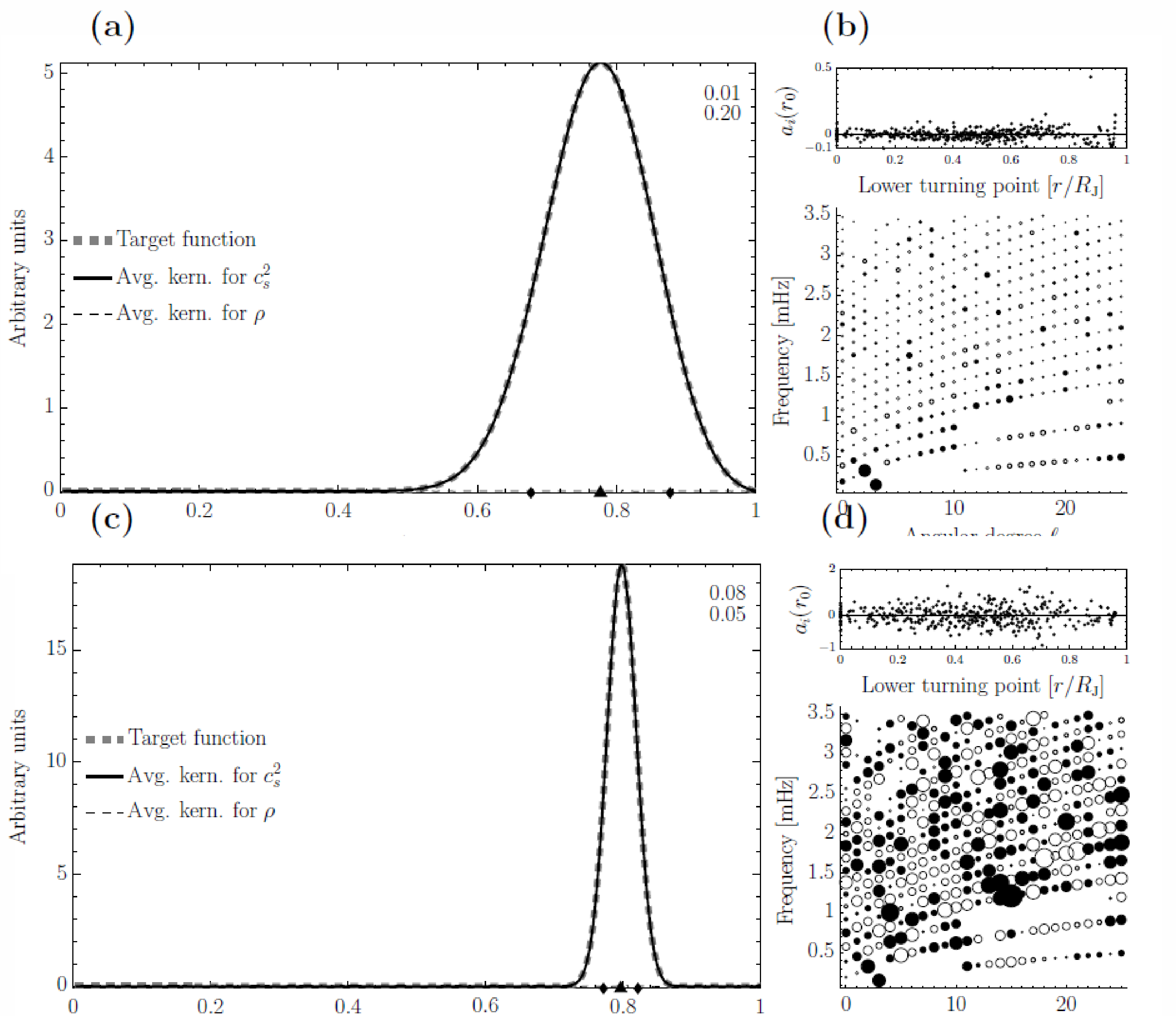

Inversion Trouble

Limited by the number of observed modes

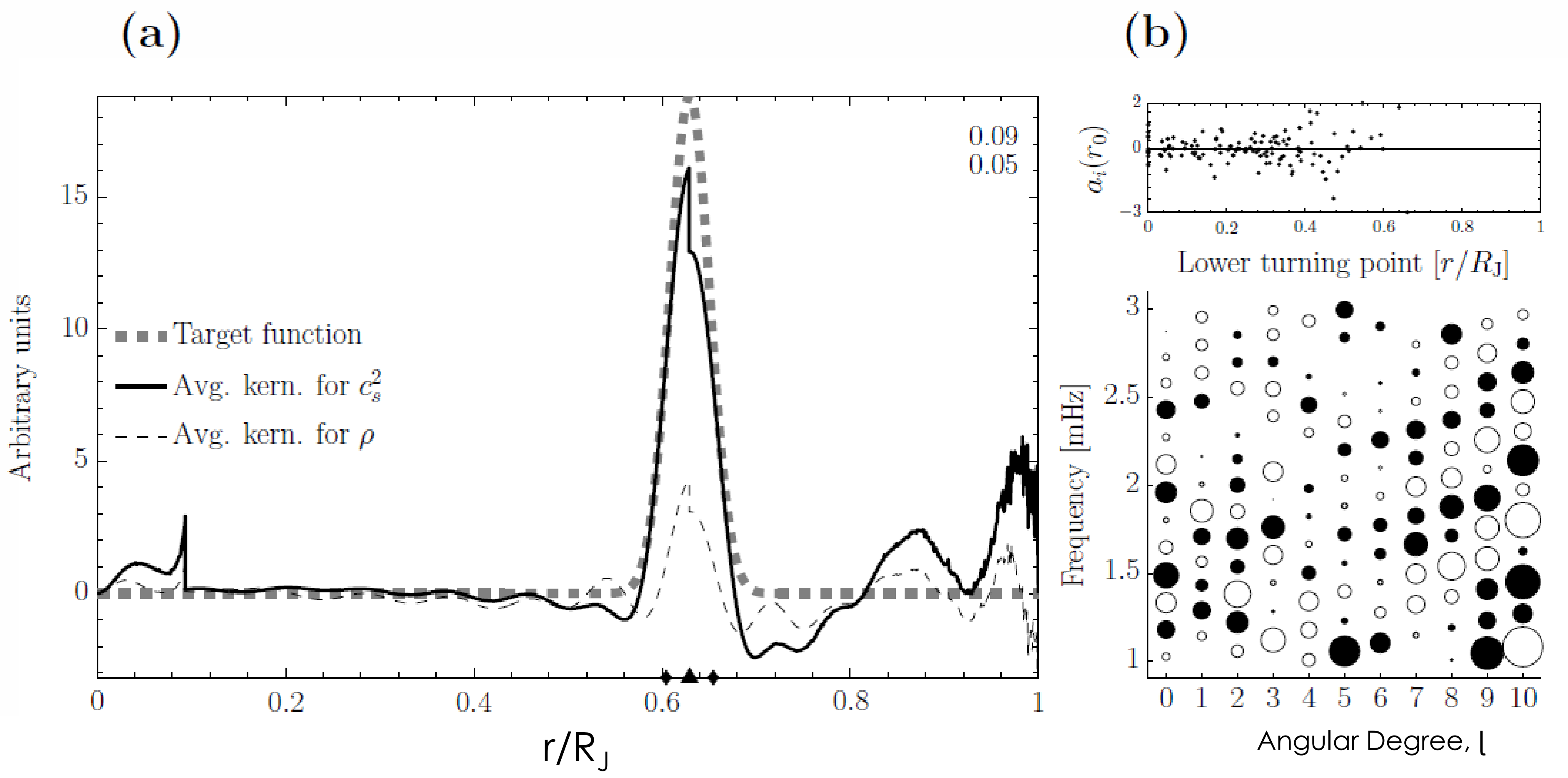

Taken from Jackiewicz et al. 2012

Conclusion

1. Derive Kernel expressions
2. Create sophisticated Saturn model
3. Compute eigenfunctions and eigenfrequencies
4. Perform inversions
5. Check if the results are within acceptable errors
6. Repeat

- Progress is on schedule and should be complete by March 2018
- Once we receive Jupiter observations we can quickly repeat for Jupiter